STM JOURNALS

Journal of
Polymer & Composites

https://journals.stmjournals.com/jopc

ISSN: 2321-2810 (Online)
ISSN: 2321-8525 (Print)
Volume 14, Special Issue 2, 2026
DOI (Journal): 10.37591/JoPC

Research JoPC

Machinability and Reliability Analysis of Al6063–Al_2O_3 Metal Matrix Composites Using Image-Based Flank Wear Evaluation

K. Usha[1], S. Gajanana[2,*], Pranav Ravindrannair[3]

Abstract

This study explores the machinability and reliability characteristics of Al6063–Al_2O_3 metal matrix composites (MMCs) as analogues for polymer–metal hybrid composite systems, focusing on their potential use in lightweight structural and metal matrix composite-integrated applications. The composite specimens were fabricated through stir casting with 3% and 9% Al_2O_3 reinforcements, followed by mechanical characterization that confirmed significant enhancements in hardness and strength compared to unreinforced Al6063. Machining experiments were performed using a high-speed steel (HSS) single-point cutting tool on a conventional lathe, applying the Taguchi design of experiments with five control factors—cutting speed, feed rate, depth of cut, rake angle, and reinforcement content, each varied at two levels. The material removal rate (MRR) and flank wear were quantitatively analyzed, with the latter evaluated using MATLAB-based image processing techniques to assess wear morphology and interface degradation. Results revealed that higher speeds and feeds yielded improved MRR, whereas lower cutting conditions promoted tool reliability by minimizing flank wear. These outcomes establish a correlation between machining reliability and reinforcement fraction, reflecting behavior similar to polymer matrix composites under tribo-mechanical stress. The study provides valuable insights for extending machinability optimization and surface integrity control to hybrid metal matrix composite structures used in aerospace and automotive manufacturing.

Keywords: HSS, single point cutting tool, image processing, Taguchi DoE, reliability

INTRODUCTION

Aluminium alloy 6063 (Al6063) is an aluminum–magnesium–silicon-based alloy widely recognized for its excellent combination of strength, ductility, corrosion resistance, and extrudability. These characteristics make it a preferred material in structural, automotive, and aerospace applications, especially where weight reduction and surface finish are crucial. In recent years, the alloy has also attracted interest as the metallic phase in polymer–metal hybrid composites, which combine the stiffness and thermal conductivity of metals with the formability and damping behavior of metal matrix composite. Understanding the machinability and reliability of Al6063 and its reinforced composites, therefore, provides critical insights for the design and performance optimization of polymer–metal hybrid structures used in advanced manufacturing.

Machinability and tool performance are governed by complex interactions among material properties, reinforcement phases, and cutting parameters. Tool wear mechanisms, such as crater

***Author for Correspondence**
S. Gajanana

[1]Professor, Department of Electronics and Communication Engineering, MVSR Engineering College, Hyderabad, Telangana, India
[2]Professor, Department of Mechanical Engineering, MVSR Engineering College, Hyderabad, Telangana, India
[3]Assistant Professor, Department of Automobile Engineering, MVSR Engineering College, Hyderabad, Telangana, India

Received Date: November 08, 2025
Accepted Date: November 20, 2025
Published Date: April 02, 2026

Citation: K. Usha, S. Gajanana, Pranav Ravindrannair. Machinability and Reliability Analysis of Al6063–Al_2O_3 Metal Matrix Composites Using Image-Based Flank Wear Evaluation. Journal of Polymer & Composites. 2026; 14(Special Issue 2): S264–S290p.

formation, built-up edge, and flank or nose wear, significantly influence surface quality and interface adhesion in both metal matrix composites. Excessive tool degradation not only reduces dimensional accuracy but also alters the thermal and tribological behaviour of the machined surface, which can impair composite bonding and coating uniformity in hybrid applications.

Several researchers have examined the statistical nature of tool wear and reliability to improve predictability in machining processes. Wager et al. [1] showed that tool life distributions in high-speed steel (HSS) cutting of low-carbon steels deviate from normality, demonstrating the stochastic nature of wear mechanisms. Hitomi et al. [2] introduced a dependability-based framework for estimating cutting tool reliability under specific machining conditions, while Lin [3] extended this approach to high-speed machining (HSM), highlighting the variance in tool wear and failure probabilities. El Wardany et al. [4] developed a stochastic model for ceramic tools, relating tool failure rate to chemical wear, progressive abrasion, and early chipping phenomena, principles also applicable to the degradation of composite machining interfaces.

In their reliability assessment of cutting tools, Salonitis et al. [5] emphasized that predicting remaining tool life is complex because tools experience multiple operations under varying parameters. The use of reliability-based design principles allows engineers to evaluate component and tooling performance under stochastic environments—an approach equally relevant to metal matrix composite systems, where the interface experiences coupled thermal–mechanical stresses during forming or cutting. Rodriguez et al. [6] further demonstrated that tool life distributions can often be modeled using normal functions, enabling determination of optimal replacement intervals to maintain surface quality and minimize downtime.

Complementary studies on aluminium-based composites reinforce this perspective. Hussain et al. [7] compared the mechanical and wear behavior of Al6063 and silicon carbide–reinforced systems, showing that reinforcement significantly improves strength and reduces frictional degradation. Aluminium's light weight and corrosion resistance make it an attractive substitute for steel in hybrid and polymer composite structures, where maintaining structural efficiency while reducing mass is critical. Bhaskar et al. [8] introduced a reliability-based method to estimate the optimal tool replacement time, and Zerti et al. [9] applied the Taguchi approach to optimize machining parameters for improved surface finish, both demonstrating the integration of statistical and experimental frameworks for process optimization.

Given these insights, the present study investigates the machinability and reliability of Al6063– Al_2O_3 composites using an HSS single-point cutting tool as a case study for metal–matrix hybrid composite analogues. By coupling Taguchi design of experiments (DoE) with image-processing-based flank wear analysis [10], the work aims to establish quantitative relationships between machining parameters, material removal rate, and tool wear reliability. The outcomes contribute to a deeper understanding of surface integrity and mechanical reliability in metal matrix systems and provide a foundation for future work on hybrid polymer–metal composite interfaces, where surface durability and consistency are paramount.

MATERIAL USED: AL6063

Aluminium alloy 6063 (Al6063) is an aluminium–magnesium–silicon (Al–Mg–Si) based alloy renowned for its exceptional corrosion resistance, excellent surface finish, and high formability [15] [16]. It exhibits a balanced combination of moderate strength, ductility, and thermal conductivity, making it ideal for structural and functional applications where lightweight design and surface integrity are essential. Typical alloying constituents include magnesium (0.45%), silicon (0.2–0.3%), iron (0.1%), copper (0.1%), zinc (0.05%), titanium (0.05%), manganese (0.05%), and trace amounts of chromium, with aluminium constituting the remainder [11].

ISSN: 2321-2810 (Online), ISSN: 2321-8525 (Print)

Owing to its high strength-to-weight ratio and extrudability, Al6063 is widely employed in aerospace, automotive, and architectural sectors, particularly in components where precision machining, corrosion protection, and aesthetic appeal are critical. Its fine-grained structure allows for intricate machining and forming operations, resulting in superior surface finishes that favor adhesion with polymer matrices and coatings. Consequently, Al6063 serves as a representative metallic phase in polymer–metal hybrid composite systems, where understanding its mechanical and tribological behavior under machining conditions helps in optimizing interfacial bonding, joint reliability, and post-processing surface treatments.

Metal Matrix Materials

Metal Matrix Materials (MMMs), also known as metal matrix composites (MMCs), are advanced engineered materials developed by incorporating reinforcing phases such as ceramics, carbides, or metallic particulates within a metallic matrix. This composite architecture is designed to overcome the inherent limitations of monolithic metals, such as poor wear resistance, limited stiffness, or inadequate high-temperature performance. By combining the ductility and toughness of metals with the hardness and stability of ceramic reinforcements, MMMs exhibit enhanced mechanical, thermal, and tribological properties.

The primary motivation behind developing MMMs parallels that of Polymer Matrix Composites (PMCs)—to create materials with tailored multifunctionality suited for extreme operating environments. While PMCs typically rely on polymer matrices reinforced with fibers or nanoparticles, MMMs serve as their metallic counterparts, offering superior thermal conductivity, load-bearing capacity, and resistance to abrasive wear. This complementarity has led to increasing research into polymer–metal hybrid composite systems, where metallic and polymeric phases are combined to achieve optimal stiffness-to-weight ratios, vibration damping, and interface durability.

The integration of reinforcements such as aluminium oxide (Al_2O_3), silicon carbide (SiC), or graphite within aluminium or magnesium matrices has proven effective in improving mechanical strength, hardness, and dimensional stability. These enhancements are critical for aerospace, automotive, and energy applications, where components are exposed to high frictional and thermal stresses. Furthermore, the interfacial bonding mechanisms between the metallic matrix and the reinforcement phase mirror the adhesion and compatibility challenges found in polymer–fiber or polymer–filler systems, underscoring the broader materials-science relevance of MMMs.

Thus, metal matrix materials not only provide an avenue for high-performance metallic composites but also offer valuable analogues for understanding hybrid composite architectures that integrate both metal and polymer constituents in modern lightweight engineering designs.

Effect of AL_2O_3 ON AL6063

Incorporating aluminium oxide (Al_2O_3) particulates into the Al6063 matrix markedly enhances its mechanical strength, hardness, and wear resistance, owing to the synergistic effect between the ductile metallic matrix and the hard ceramic reinforcement. Al_2O_3 acts as a load-bearing and wear-resistant phase, improving the composite’s ability to withstand mechanical deformation, frictional stress, and thermal softening during service or machining.

Uniform dispersion of Al_2O_3 particles within the aluminium matrix is critical to achieving consistent performance. The reinforcement particles impede grain growth during solidification and heat exposure, resulting in refined microstructures that display elevated micro hardness and compressive strength. Additionally, these ceramic particulates act as obstacles to dislocation motion, contributing to increased yield strength and improved dimensional stability under cyclic loads.

However, the presence of rigid Al_2O_3 particles slightly reduces the alloy’s toughness and ductility, as the reinforcement limits plastic deformation pathways within the matrix. This transition toward a more brittle fracture response resembles behavior observed in polymer matrix composites where the incorporation of stiff fillers or fibers enhances stiffness and wear resistance but may compromise impact strength. The parallel between metallic and polymeric composite systems underscores the universal role of reinforcement–matrix interaction in dictating mechanical balance.

From a tribological perspective, the Al_2O_3 phase forms a protective interfacial barrier during sliding or cutting conditions, thereby minimizing adhesive wear and surface damage. Under moderate loads, this leads to a notable reduction in the wear rate. However, at higher contact stresses, localized strain concentrations at the reinforcement–matrix interface may induce microcrack initiation or particle pull-out, analogous to fiber–matrix debonding phenomena seen in polymer–fiber composites. The overall performance of Al6063– Al_2O_3 thus depends strongly on the uniformity and integrity of the interfacial bonding, which governs load transfer efficiency, wear resistance, and fatigue reliability.

Methodology and Work Material Preparation

The experimental methodology was designed to systematically evaluate the machinability and reliability characteristics of Al6063– Al_2O_3 composites, with particular attention to optimizing their mechanical and surface response under controlled cutting conditions. The procedure consisted of three key stages: material synthesis, compositional optimization using the Taguchi design of experiments (DoE), and machinability testing using a single-point cutting tool.

Preparation and Optimization of The Al6063 Base Alloy

The base matrix of Al6063 was first prepared with optimized elemental composition to achieve high mechanical strength and process stability. The alloying elements—magnesium, silicon, and trace constituents such as Fe, Cu, Zn, and Ti—were selected according to standard specifications [18] [19] [20] and refined to minimize casting defects and ensure homogeneity. The composition of each material is given in Table 1. The Taguchi DoE approach was employed to determine the most influential process factors affecting strength and hardness during the stir casting process, a method chosen for its uniform reinforcement dispersion and repeatable quality.

Fabrication of Metal Matrix Composites (MMCS)

Two composite formulations were developed by reinforcing the Al6063 matrix with 3 wt.% and 9 wt.% of Al_2O_3 particulates, based on prior literature and pilot trials indicating their effectiveness in improving wear resistance without excessive brittleness. The samples preparation is shown in Figure 1. The stir casting method was employed to ensure uniform particle distribution. The molten Al6063 alloy was maintained at an optimal temperature to prevent oxidation, and preheated Al_2O_3 particulates were introduced under mechanical stirring to enhance wetting and interfacial bonding. The cast composites were allowed to solidify under controlled cooling to minimize porosity and segregation [13][16].

Table 1. Composition of material used,

Material	Mg	Si	Fe	Cu	Zn	Ti	Mn	Cr	Al
Wt%	0.45	0.2	0.3	0.1	0.1	0.05	0.05	0.1	98.65

Figure 1. Preparation of samples for machining.

Machinability Investigation

The prepared Al6063– Al_2O_3 composites were subjected to machinability testing using a high-speed steel (HSS) single-point cutting tool. This tool material was selected for its compatibility with aluminium-based composites and its well-characterized wear mechanisms, which facilitate quantitative reliability analysis. The machining trials were conducted under varying parameters of cutting speed, feed rate, and depth of cut, rake angle, and reinforcement percentage, structured through a Taguchi L16 orthogonal array. These trials aimed to correlate material removal rate (MRR) and flank wear with the input variables, providing a foundation for establishing a reliability-based machinability model.

The adopted methodology ensures a systematic, statistically valid exploration of machining behavior, while the analysis of flank wear through image processing techniques provides high precision in assessing surface degradation. Such an approach not only contributes to understanding metal matrix machinability but also offers insights applicable to polymer–metal hybrid composites, where interfacial wear, bonding reliability, and surface integrity are equally critical for functional performance.

EXPERIMENTAL DESIGN USING THE TAGUCHI METHOD

The Taguchi design of experiments (DoE) approach was employed to systematically evaluate the influence of multiple process parameters on the machinability and reliability of Al6063–Al_2O_3 composites. This methodology is widely recognized for its robustness and efficiency in identifying key control factors with a minimal number of experimental trials, thereby optimizing both cost and time while maintaining statistical precision.

For this investigation, five process parameters were selected based on their established significance in determining material removal efficiency, surface integrity, and tool wear behavior [12]:

- *Cutting speed (rpm):* A primary factor influencing heat generation, chip formation, and tool wear rate.
- *Feed rate (mm/rev):* Determines the material removal rate (MRR) and surface roughness of the machined composite.
- *Depth of cut (mm):* Directly affects cutting forces, thermal load, and tool life.
- *Rake angle (°):* Governs chip flow, contact pressure, and the effective cutting geometry of the tool.
- *Reinforcement composition (% Al_2O_3):* Modifies the composite's hardness, wear response, and thermal conductivity, thereby influencing machinability. [17]

Each parameter was investigated at two distinct levels, representing practical and industrially relevant operating ranges. To efficiently explore the parameter space while capturing the primary effects and interactions, a Taguchi L16 orthogonal array was adopted. This array structure ensures balanced and orthogonal representation of the experimental variables, enabling independent assessment of each factor's contribution to the output responses. The complete details of experimental design and setup are given in Table 2.

The selection of the Taguchi method in this context is particularly relevant to composite material optimization, as it parallels approaches used in polymer matrix and hybrid composites where multiple factors, such as filler loading, fiber orientation, and processing temperature, collectively determine mechanical and tribological performance. By applying this statistical framework, the present study establishes a quantitative link between process parameters and machinability outcomes, facilitating predictive modeling of tool reliability and surface quality in Al6063– Al_2O_3 composites.

The experimental design thus forms the analytical foundation for evaluating how reinforcement fraction and cutting parameters influence key performance metrics, including material removal rate (MRR) and flank wear progression, both of which are critical to understanding interfacial reliability and surface integrity in advanced composite and hybrid material systems.

Table 2. Experimental design and setup.

Trail no	Speed (RPM)	Feed (mm/rev)	DOC (mm)	Rake angle (degrees)	Composition	Tool no
1	285	0.287	0.3	15	3%	1
2	285	0.287	0.5	20	3%	1
3	285	0.527	0.3	20	3%	2
4	285	0.527	0.5	15	3%	2
5	640	0.287	0.3	20	3%	3
6	640	0.287	0.5	15	3%	3
7	640	0.527	0.3	15	3%	4
8	640	0.527	0.5	20	3%	4
9	285	0.287	0.3	20	9%	5
10	285	0.287	0.5	15	9%	5
11	285	0.527	0.3	15	9%	6
12	285	0.527	0.5	20	9%	6
13	640	0.287	0.3	20	9%	7
14	640	0.287	0.5	15	9%	7
15	640	0.527	0.3	20	9%	8
16	640	0.527	0.5	15	9%	8

Each selected parameter was examined at two distinct levels, representing practical variations typically observed in machining operations of composite and hybrid materials. These levels were determined through pilot studies and supported by literature on aluminium-based and metal matrix composite systems.

By applying this orthogonal array, the study establishes a robust statistical foundation for analyzing machinability, reliability, and interfacial response, bridging the methodological principles used in metal matrix composites (MMCs).

WORKPIECE PREPARATION

The casted Al6063– Al_2O_3 composite specimens were machined to the required dimensions in order to remove surface irregularities and achieve uniform geometry suitable for experimental testing. Machining, a conventional subtractive manufacturing process, was employed to shape the specimens accurately by selectively removing material from the cast blanks. Despite being one of the oldest fabrication techniques, machining remains indispensable in applications demanding high dimensional accuracy, superior surface finish, and controlled surface integrity, especially for composite and hybrid materials.

A Engine lathe was utilized for all machining operations to ensure precision and repeatability under controlled conditions. The composite workpieces, after casting, were turned to achieve a final length of 140 mm and a diameter of 22 mm, ensuring consistent surface conditions across all experimental trials. Grooving operations were subsequently performed using a grooving tool at 25 mm intervals along the specimen length to create discrete machining zones corresponding to different parameter combinations in the Taguchi design.

This structured machining procedure ensured a standardized contact surface for the cutting tool and minimized geometric or surface-related variability among samples. Moreover, maintaining uniform geometry and surface finish is critical not only for accurate machinability and wear analysis but also for establishing parallels with –metal matrix hybrid systems, where surface morphology directly affects adhesion strength, interface bonding, and load transfer efficiency.

A schematic representation of the machined workpiece geometry and grooving layout is shown in Figure 2.

Figure 2. Workpiece after grooving.

EXPERIMENTATION

The machining experiments were conducted on a centre lathe equipped with a three-component dynamometer, designed to record cutting forces during turning operations [11]. Two categories of specimens were prepared: the Al6063 base alloy and Al6063 reinforced with Al_2O_3 particulates (3% and 9%), enabling comparative analysis of reinforcement influence on machinability and reliability. The experimental setup and experimentation are shown in Figure 3 and Figure 4.

The procedure was executed systematically in the following stages to ensure precision, repeatability, and consistent data acquisition:

Step 1: Specimen Preparation and Setup

The initial weight of each specimen was recorded using a precision balance to establish a baseline for subsequent material removal measurements. The cylindrical workpiece was then securely mounted in the lathe chuck, ensuring proper concentric alignment to minimize vibration. The HSS single-point cutting tool, pre-set to the designated rake angle, was clamped in the toolpost and positioned to maintain uniform tool–work engagement across all trials.

Step 2: Parameter Configuration and Machining

Machining parameters were configured based on the Taguchi L16 orthogonal array, covering all predefined combinations of cutting speed, feed rate, depth of cut, rake angle, and reinforcement composition. Each trial involved machining a 50 mm section along the specimen's length. The cutting conditions were carefully maintained to ensure consistent thermal and mechanical exposure of the tool–work interface.

Step 3: Monitoring and Data Acquisition

During each machining run, the operation time was recorded using a stopwatch to facilitate accurate calculation of the material removal rate (MRR). Concurrently, the cutting forces (F_x, F_y, and F_z) were continuously monitored and logged using the lathe-mounted dynamometer. Chip morphology and formation patterns were observed, and chips were collected after each trial to quantify the mass of material removed.

Figure 3. Experimental setup.

Figure 4. Experimentation.

Step 4: Post-Machining Measurements

Upon completion of each experiment, the final weight of the machined workpiece and the mass of the collected chips were measured. These measurements were used to compute the MRR, providing a quantitative basis for comparing machining efficiency under different parameter combinations. Surface observations were also made to evaluate potential variations in texture and tool interaction.

Step 5: Repetition and Parameter Variation

Following each trial, the workpiece was re-mounted, and the next set of Taguchi-design parameters was applied. This systematic, sequential approach ensured that all 16 experimental combinations were executed under identical environmental conditions, thus minimizing external variability.

This controlled methodology not only enabled accurate assessment of machinability and tool performance but also ensured the reproducibility of data for reliability analysis [12]. The collected results form the foundation for understanding the interaction between reinforcement fraction, tool geometry, and process parameters, offering insights applicable to polymer–metal hybrid systems, where similar interfacial and tribological interactions govern performance and durability.

Table 3. Observations for the composition Al6063+Al_2O_3.

Trail no	Rake angle (degrees)	Weight before (gms)	Weight after (gms)	W1-W2 (gms)	Machining time (s)	MRR (gms/s)
1	15	136.83	135.09	1.74	74	1.41
2	20	135.09	133.29	1.8	81	1.33
3	20	133.29	130.83	2.46	103	14.33
4	15	130.83	130.44	0.39	10.6	2.21
5	20	133.78	131.36	2.42	4.5	32.27
6	15	131.36	130.31	1.05	4.79	13.15
7	15	130.31	127.77	2.54	4.97	30.66
8	20	127.77	125.19	2.58	4.89	31.66
9	20	139.35	138.04	1.31	10.6	7.42
10	15	138.04	136.41	1.63	9.64	10.15
11	15	136.41	134.43	1.98	10.45	11.37
12	20	134.43	131.55	2.88	11.41	15.14
13	15	136.85	136.24	0.61	6.77	5.41
14	20	136.24	134.14	2.1	4.58	27.51
15	20	134.14	131.77	2.37	7.5	18.96
16	15	131.77	129.41	2.36	4.87	29.08

Journal of Polymer & Composites
Volume 14, Special Issue 2
ISSN: 2321-2810 (Online), ISSN: 2321-8525 (Print)

Experimental Observations

Table 3 summarizes the experimental observations recorded for the Al6063– Al_2O_3 composites under various machining conditions derived from the Taguchi L16 orthogonal array. Each trial was performed with a defined rake angle, and the corresponding initial and final weights of the specimens were measured to determine the material removed (W1 – W2). The material removal rate (MRR) was calculated by dividing the removed mass by the machining time for each test. The results show clear trends linking machining parameters to removal efficiency: higher cutting speeds and feeds produced greater MRR values, while lower speeds and smaller feeds tended to reduce removal rates but enhanced tool stability. Variations in rake angle also influenced the chip formation behavior and heat dissipation at the tool–work interface. These quantitative observations formed the basis for subsequent analysis of flank wear, tool reliability, and surface integrity, providing valuable insight into the interfacial performance of metal matrix and polymer–metal hybrid composite systems under different machining regimes.

Observations of Flank Wear (VB)

For all the 16 trials flank wear is observed after each trial and are shown in Figure 5 to Figure 20

Trial 1

Speed = 285 rpm. Feed = 0.287 mm/rev. Depth of Cut = 0.3 mm. Rake Angle = 15° Composition = 3%AL_2O_3

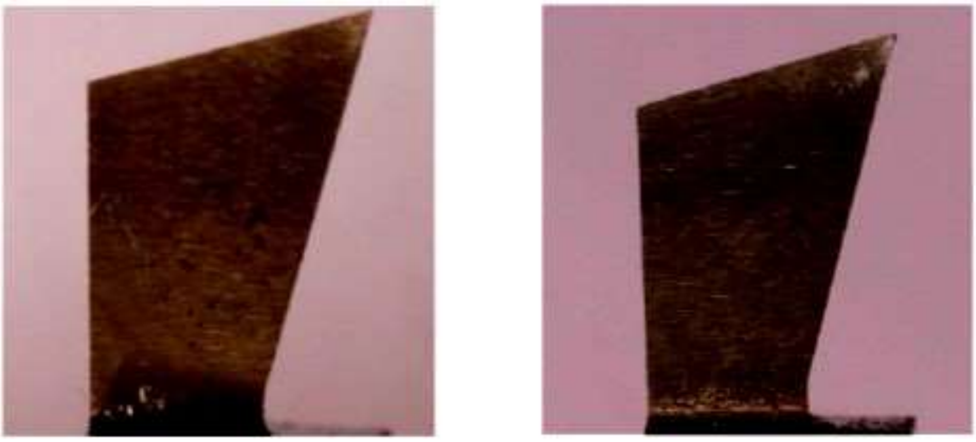

Figure 5. Tool-1(15°) geometry before and after experiment.

Trial 2:

Speed = 285 rpm, Feed = 0.287 mm/rev. Depth of Cut = 0.5 mm. Rake Angle = 20°. Composition = 3% Al2O

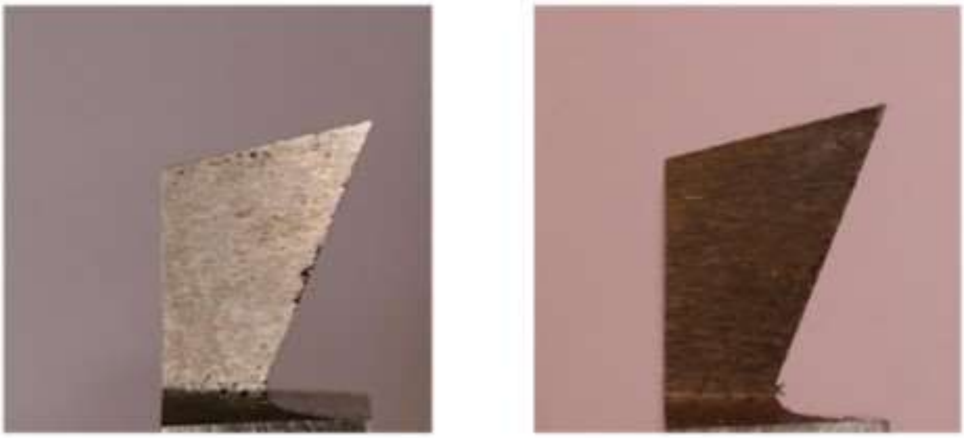

Figure 6. Tool-1(20°) geometry before and after experiment.

Trial 3:

Speed = 285 rpm, Feed = 0.527 mm/rev, Depth of Cut= 0.3 mm. Rake Angle = 20°,

Figure 7. Tool-2(20°) geometry before and after experiment.

Trial 4:

Speed = 285 rpm. Feed = 0527 mm/rev Depth of Cut= 05 mm. Rake Angle 15°

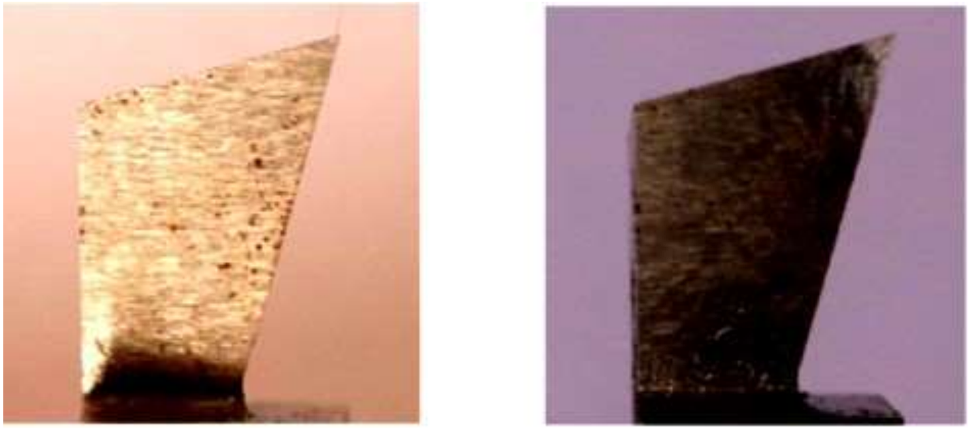

Figure 8. Tool-2(15°) geometry before and after experiment.

Trial 5:

Speed = 640 rpm. Feed = 0.287 mm/rev. Depth of Cut= 0.3 mm. Rake Angle = 20°

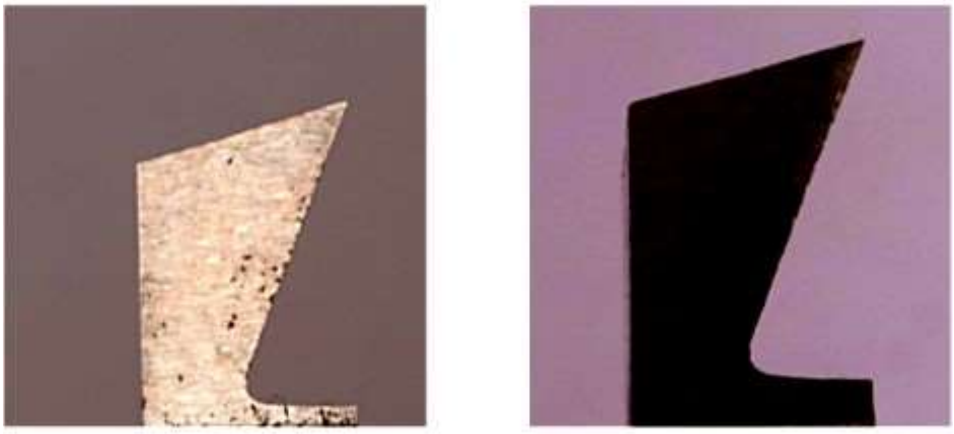

Figure 9. Tool-3(20°) geometry before and after experiment.

Trial 6:

Speed = 640 rpm. Feed = 0.287 mm/rev Depth of Cut= 05 mm. Rake Angle = 15° Composition 3% Al_2O_3

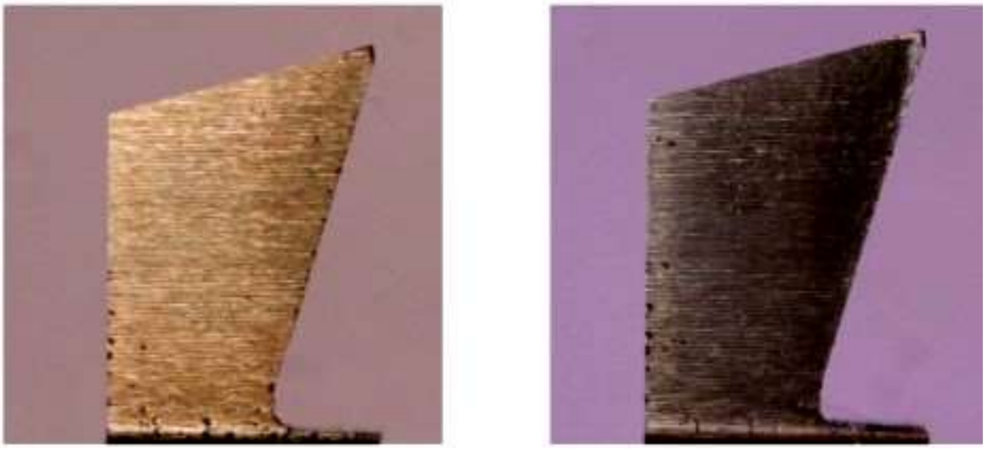

Figure 10. Tool-3(15°) geometry before and after experiment.

Trial 7:

Speed = 640 rpm, Feed = 0.527 mm/rev, Depth of Cut = 0.3 mm. Rake Angle =15°Composition = 3% Al_2O3

Figure 11. Tool-4(15°) geometry before and after experiment.

Trial 8:

Speed = 640 rpm, Feed = 0.527 mm/rev. Depth of Cut = 0.5 mm. Rake Angle = 20° Composition = 3% Al_2O_3

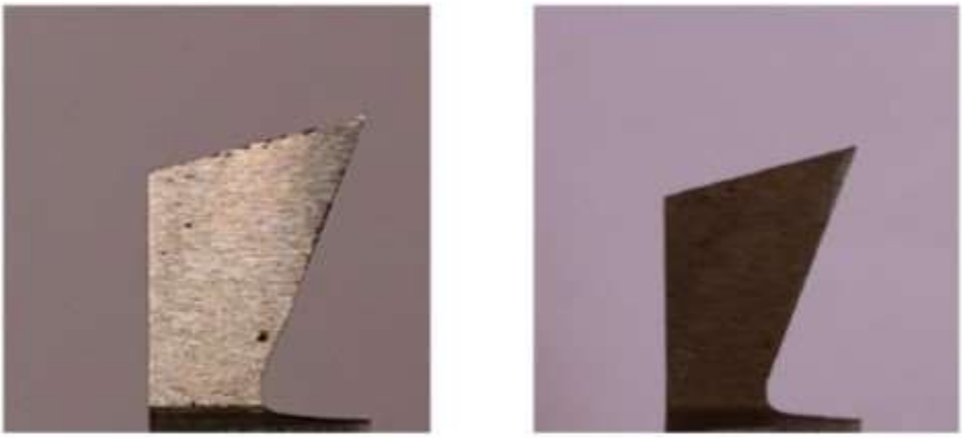

Figure 12. Tool-4(20°) geometry before and after experiment.

Trial 9:

Speed = 285 rpm, Feed = 0.287 mm/rev. Depth of Cut = 0.3 mm. Rake Angle = 20°,

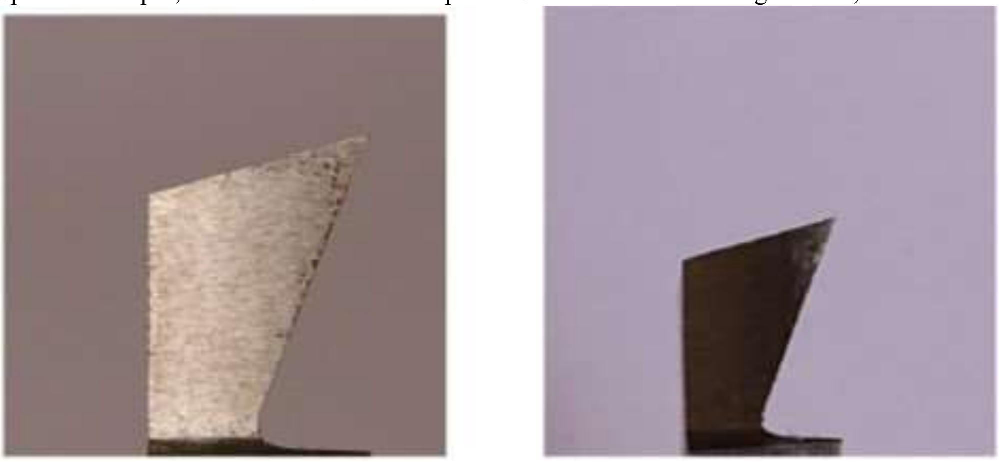

Figure 13. Tool-5(20°) geometry before and after experiment.

Trial 10

Speed = 285 rpm. Feed = 0.287 mm/rev. Depth of Cut = 0.5 mun. Rake Angle = 15°.

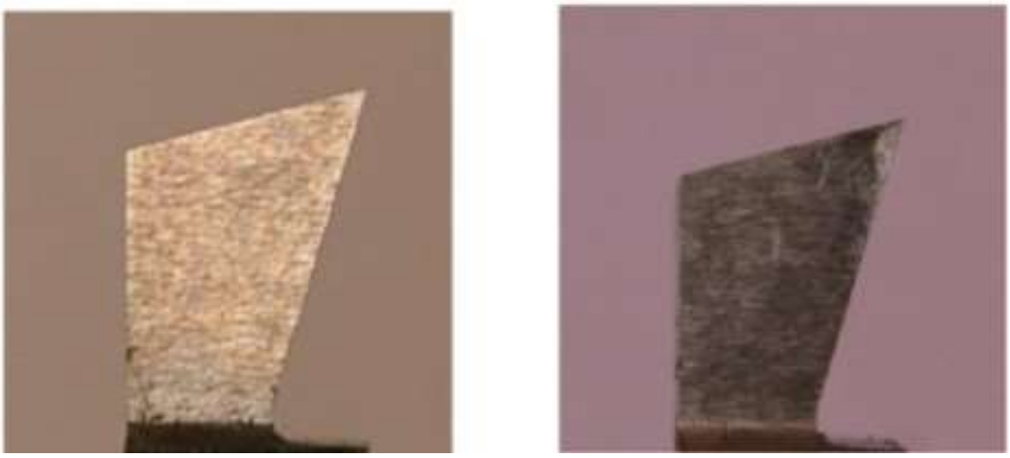

Figure 14. Tool-5(15°) geometry before and after experiment.

Trial 11:

Speed = 285 rpm, Feed = 0.527 mm/rev, Depth of Cut = 0.3 mm. Rake Angle =15. Composition = 9% Al_2O_3

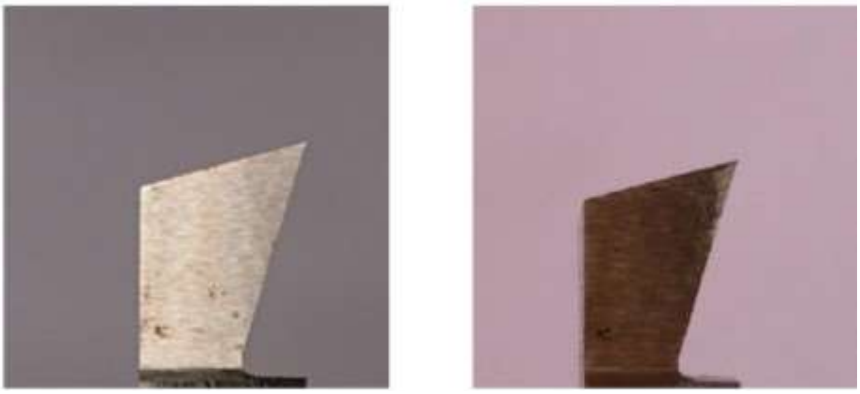

Figure 15. Tool-6(15°) geometry before and after experiment.

Journal of Polymer & Composites
Volume 14, Special Issue 2
ISSN: 2321-2810 (Online), ISSN: 2321-8525 (Print)

Trial 12:

Speed = 285 rpm. Feed = 0.527 mm/rev. Depth of Cut = 0.5 mm. Rake Angle = 20 °,

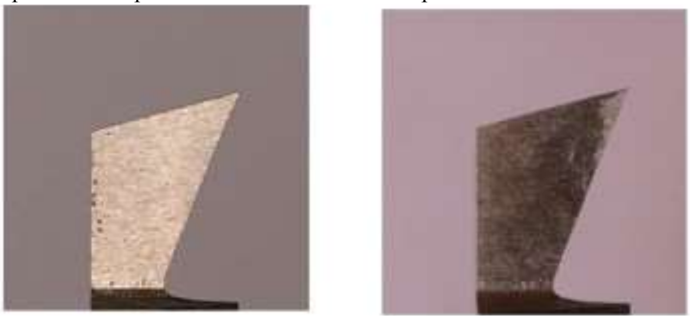

Figure 16. Tool-6(20°) geometry before and after experiment.

Trial 13

Speed = 640 rpm Feed = 0.287 mm/rev Depth of cut =0.3 mm Rake Angle =15 ° Composition = 9% Al_2O_3

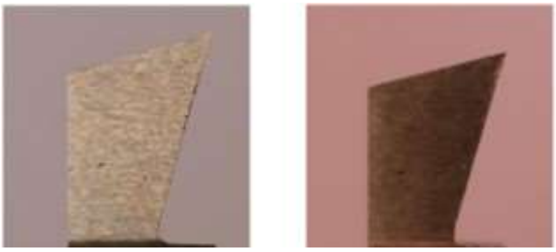

Figure 17. Tool-7(15°) geometry before and after experiment.

Trial 14:

Speed = 640 rpm, Feed = 0.287 mm/rev, Depth of Cut = 0.5 mm, Rake Angle = 20 °, Composition = 9% Al_2O_3

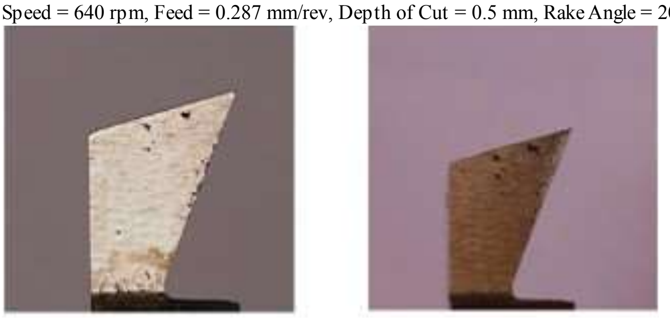

Figure 18. Tool-7(20°) geometry before and after experiment.

Trial 15:

Speed = 640 rpm, Feed = 0.527 mm/rev, Depth of Cut = 0.3 mm, Rake Angle = 20°, Composition = 9% Al_2O_3

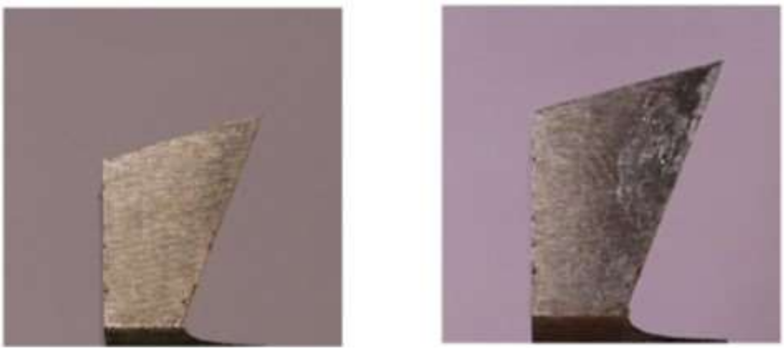

Figure 19. Tool-8(20°) geometry before and after experiment.

Trial 16:

Speed = 640 rpm, Feed = 0.527 mm/rev, Depth of Cut = 0.5 mm. Rake Angle = 15. Composition = 9% Al_2O_3

Figure 20. Tool-8(15°) geometry before and after experiment.

Calculation of flank wear using Image processing in MATLAB

Flank wear (V_B) is one of the most significant indicators of tool degradation, directly influencing machined surface quality, dimensional accuracy, and tool reliability. To achieve accurate and repeatable measurements, an image-processing-based technique was implemented using MATLAB. This approach provides a non-contact, precise, and efficient means of quantifying tool wear progression [13], overcoming the limitations of manual or optical measurement methods.

The analytical procedure followed is outlined below:

1. *Image acquisition*: High-resolution images of the cutting tool were captured after each machining trial to record the extent of flank wear. Contour Detection: The contour of the worn region was extracted using MATLAB's contour detection functions, defining the wear boundary for quantitative analysis.
2. *Reference definition*: A reference line corresponding to the original unworn tool edge was established to serve as the measurement baseline.
3. *Calibration*: A calibration factor was computed by dividing the pixel length by a known dimensional reference in the image, enabling accurate conversion from pixel to real-world units.
4. *Image conversion*: The captured image was converted to gray scale and then to a binary format to isolate the wear region and simplify edge detection.
5. *Noise filtering*: Image noise and irregularities were minimized using morphological filtering techniques to enhance the accuracy of contour extraction.
6. *Coordinate mapping*: Discrete coordinate points (x, y) were generated along the wear contour to represent the profile of the worn surface.
7. *Wear distance calculation*: The vertical distance between the worn contour and the reference edge was computed for corresponding x-values, providing localized flank wear data.
8. *Average wear determination*: The average of these distances was calculated to obtain the representative value of flank wear for each tool.
9. *Unit conversion*: The mean pixel distance was multiplied by the calibration factor to express flank wear (V_B) in millimeters.
10. *Wear profile representation*: The final wear values were plotted and tabulated to compare the extent of degradation across different machining conditions.
11. *Repetition for consistency*: The process was repeated for all tool specimens to ensure consistency and statistical reliability of the measurements.

MATLAB Results

This MATLAB-assisted image analysis as shown in Figure 21 and Figure 36 provides a high-resolution and reproducible quantification of flank wear, enabling correlation between machining parameters, wear progression, and surface quality. Moreover, the digital image-based methodology

Journal of Polymer & Composites
Volume 14, Special Issue 2
ISSN: 2321-2810 (Online), ISSN: 2321-8525 (Print)

establishes a framework applicable to polymer–metal hybrid interfaces and composite machining, where similar surface wear mapping and contour-based analysis techniques are valuable for evaluating adhesion, damage propagation, and interface reliability.

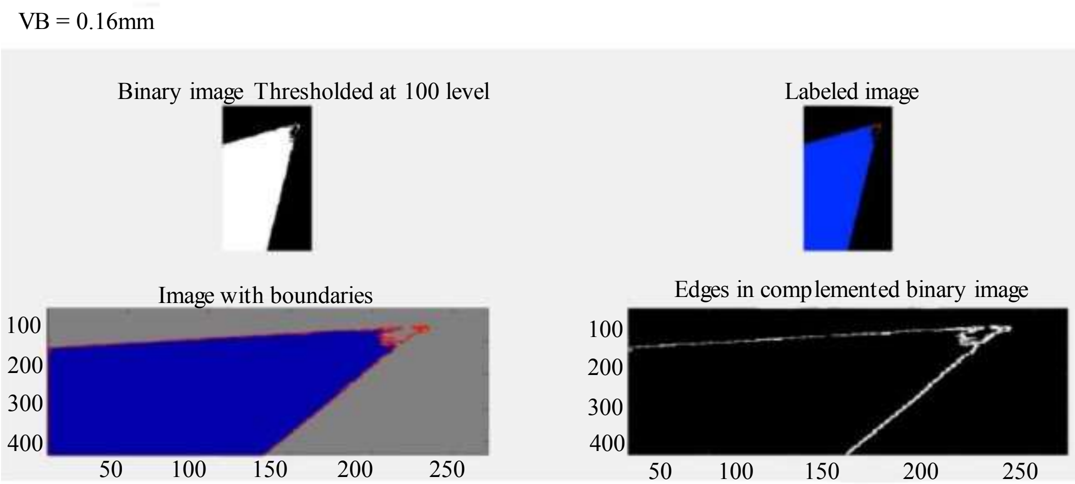

Figure 21. Flank wear MATLAB images for Trial -1.

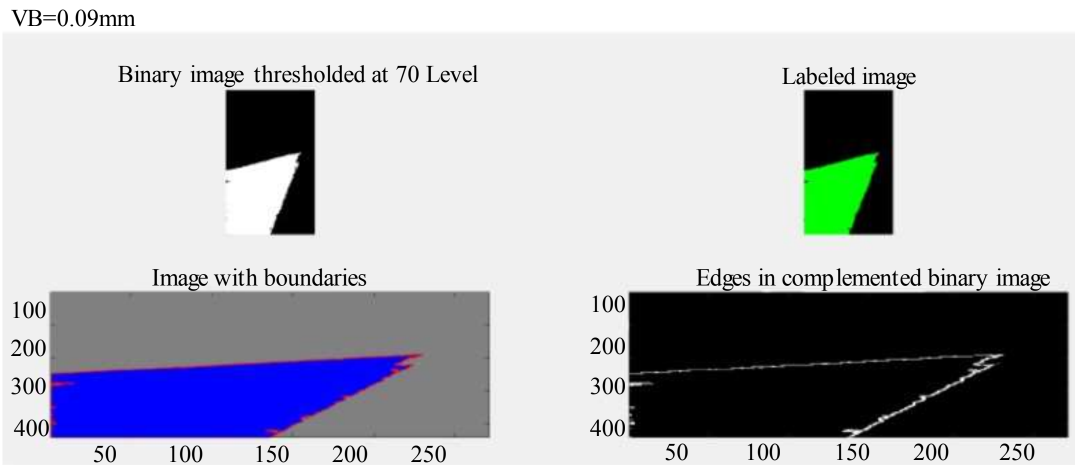

Figure 22. Flank wear MATLAB images for Trial -2.

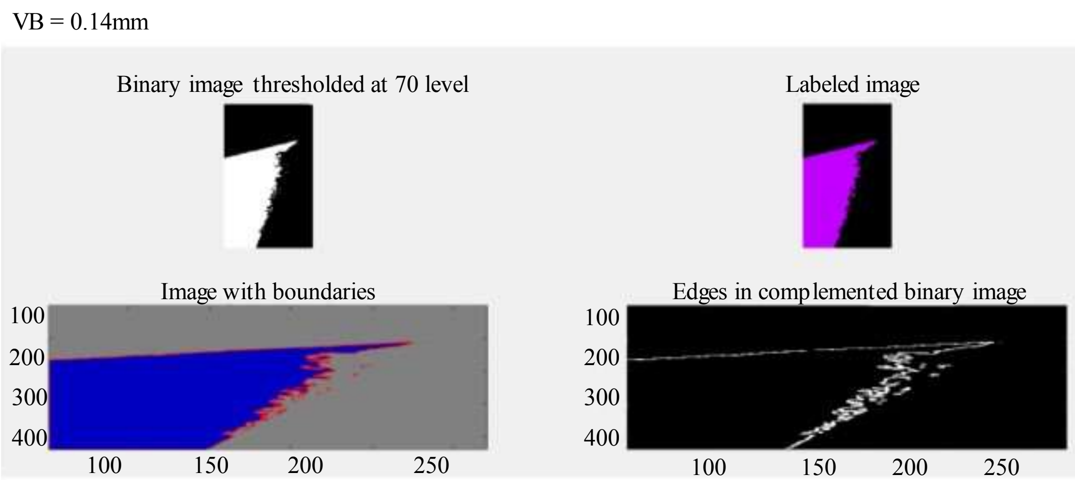

Figure 23. Flank wear MATLAB images for Trial -3.

VB = 0.18mm

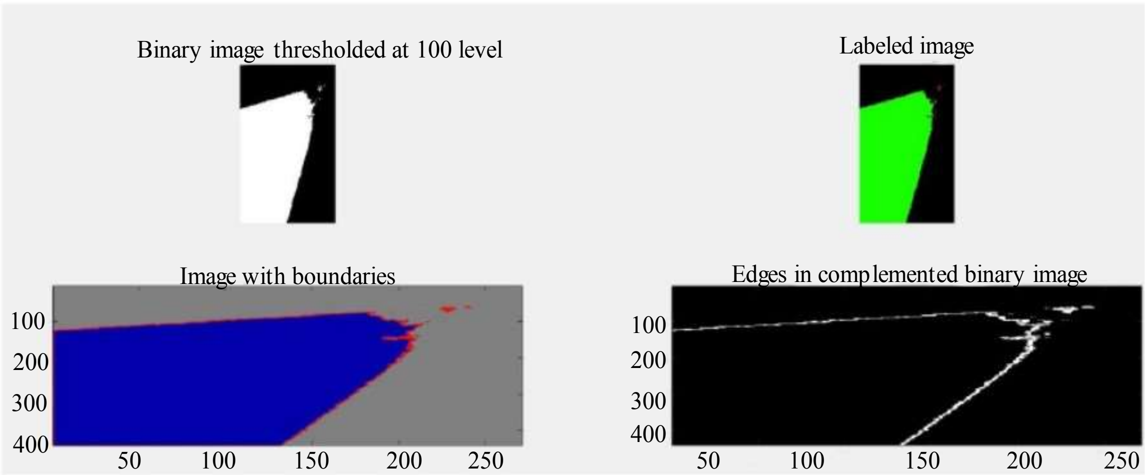

Figure 24. Flank wear MATLAB images for Trial -4.

VB-0.12mm

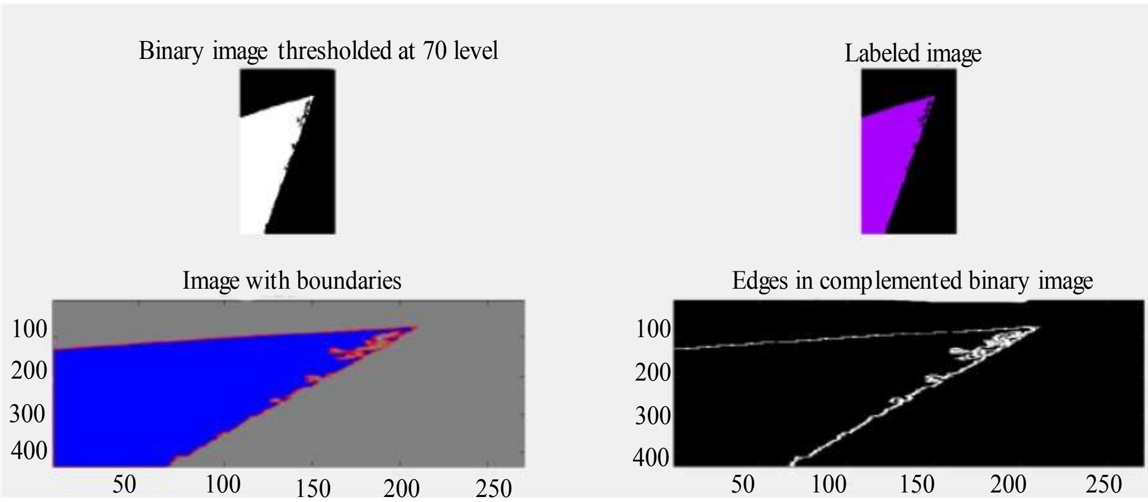

Figure 25. Flank wear MATLAB images for Trial -5.

VB = 0.13mm

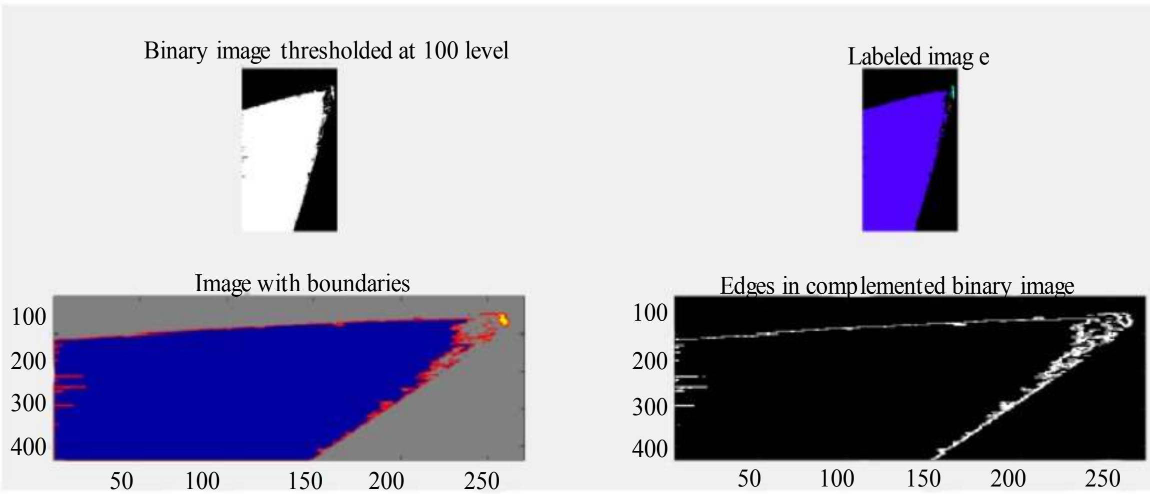

Figure 26. Flank wear MATLAB images for Trial -6.

VB = 0.157mm

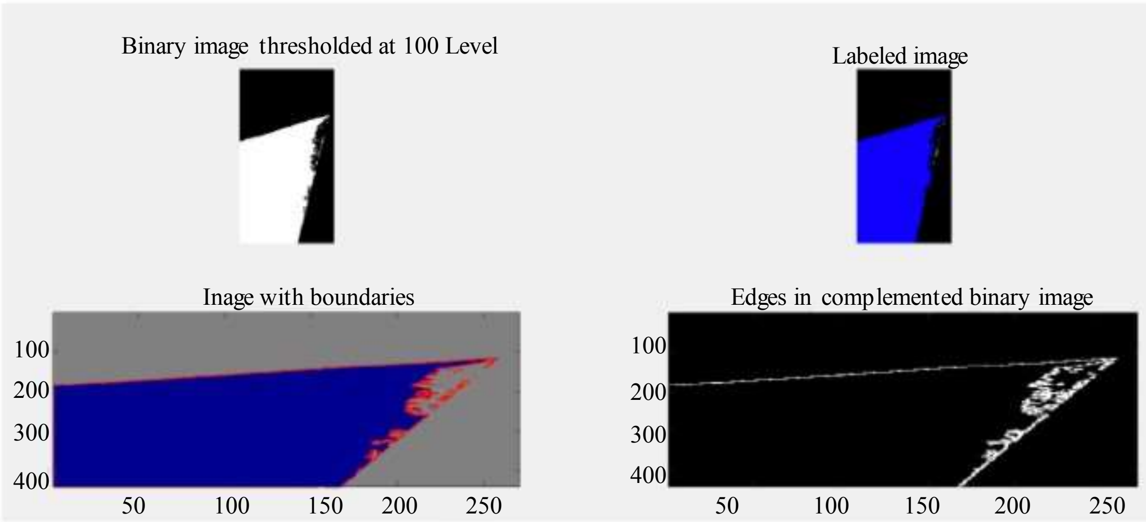

Figure 27. Flank wear MATLAB images for Trial -7.

VB = 0.1mm

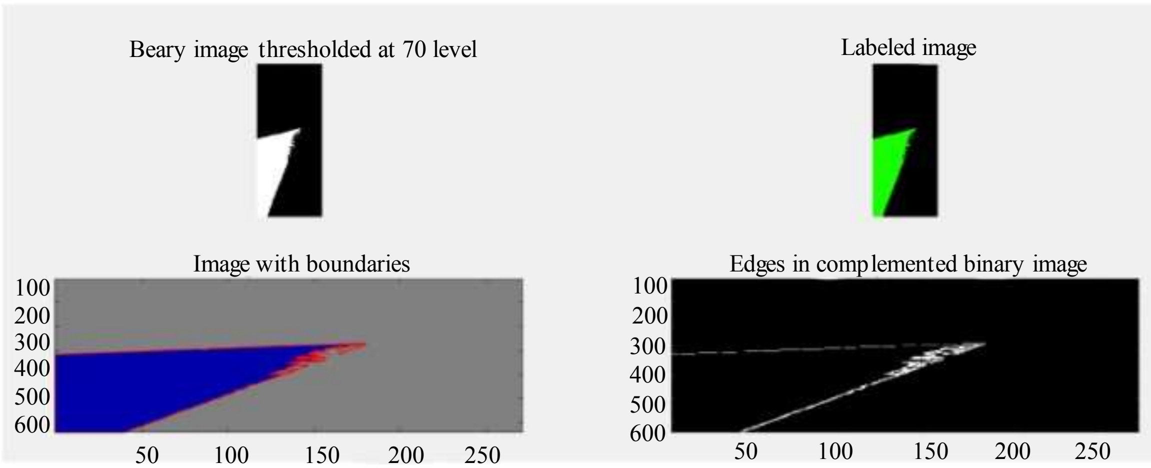

Figure 28. Flank wear MATLAB images for Trial -8.

VB = 0.17mm

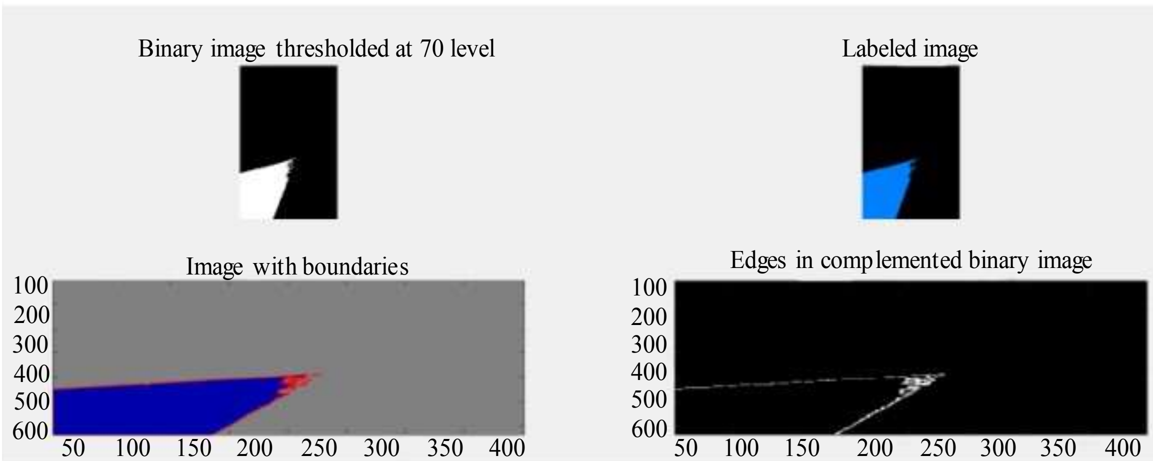

Figure 29. Flank wear MATLAB images for Trial -9.

VB = 0.12mm

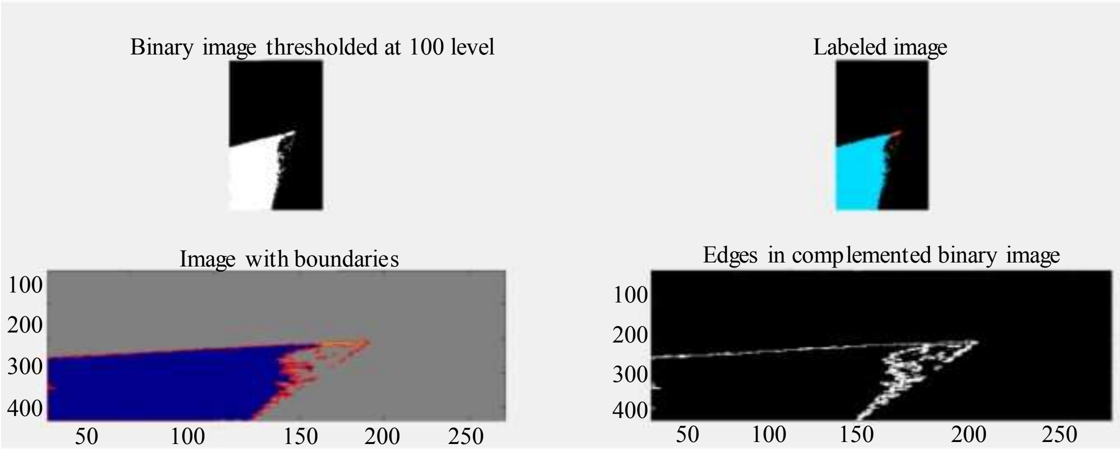

Figure 30. Flank wear MATLAB images for Trial -10.

VB = 0.134mm

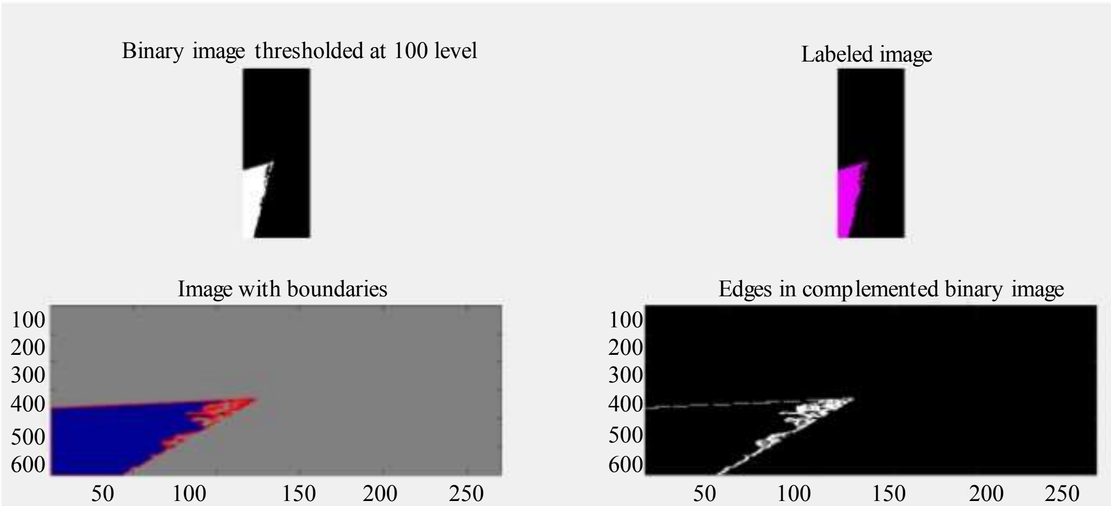

Figure 31. Flank wear MATLAB images for Trial -11.

VB = 0.1mm

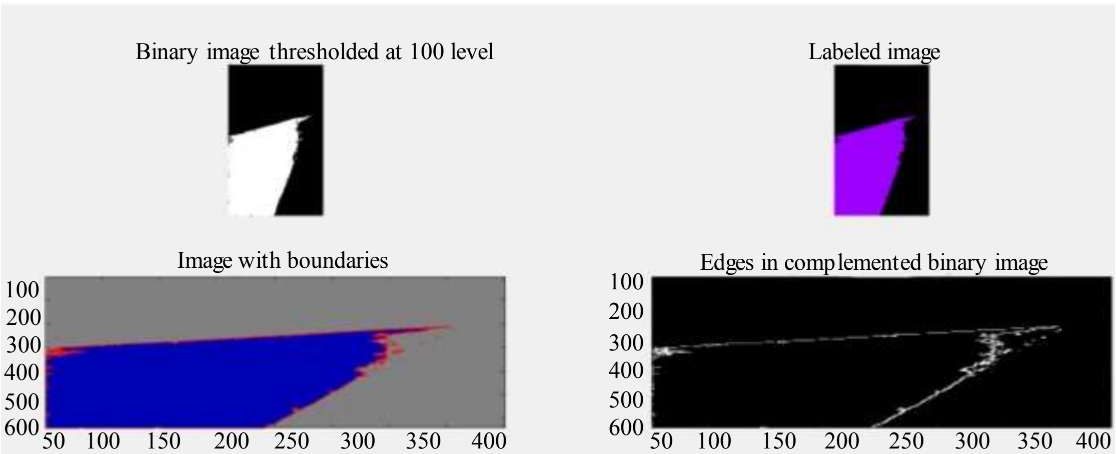

Figure 32. Flank wear MATLAB images for Trial -12.

VB = 0.08mm

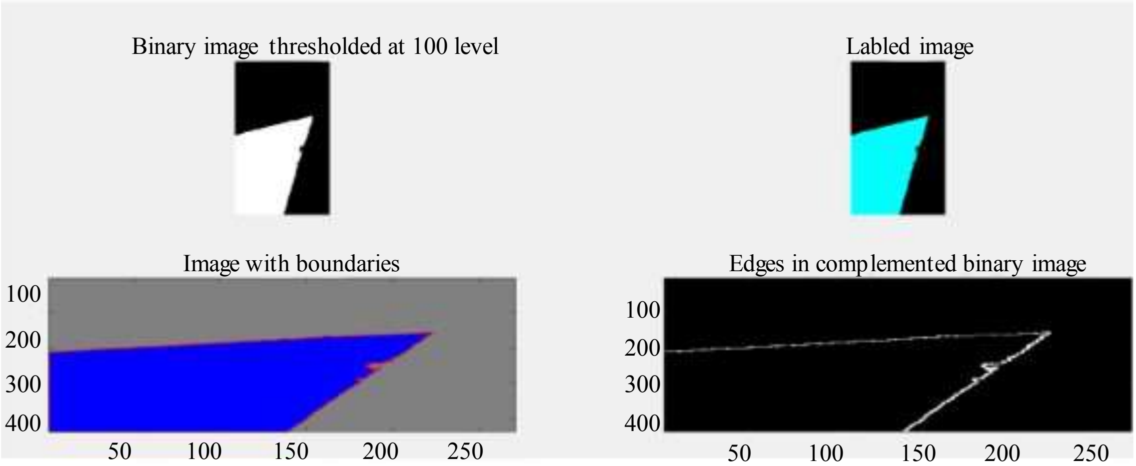

Figure 33. Flank wear MATLAB images for Trial -13.

VB = 0.07mm

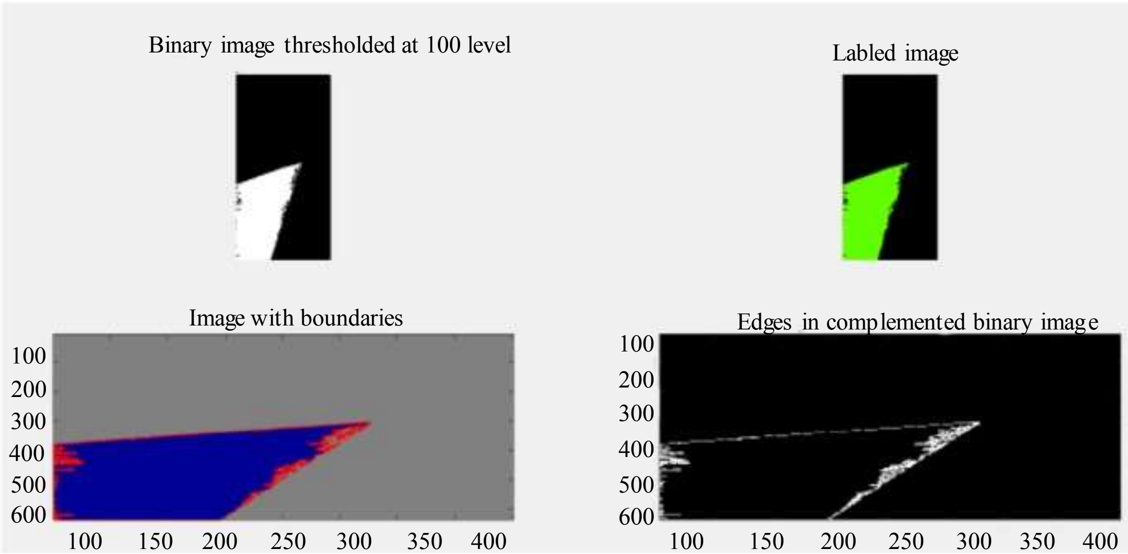

Figure 34. Flank wear MATLAB images for Trial -14.

VB = 0.11mm

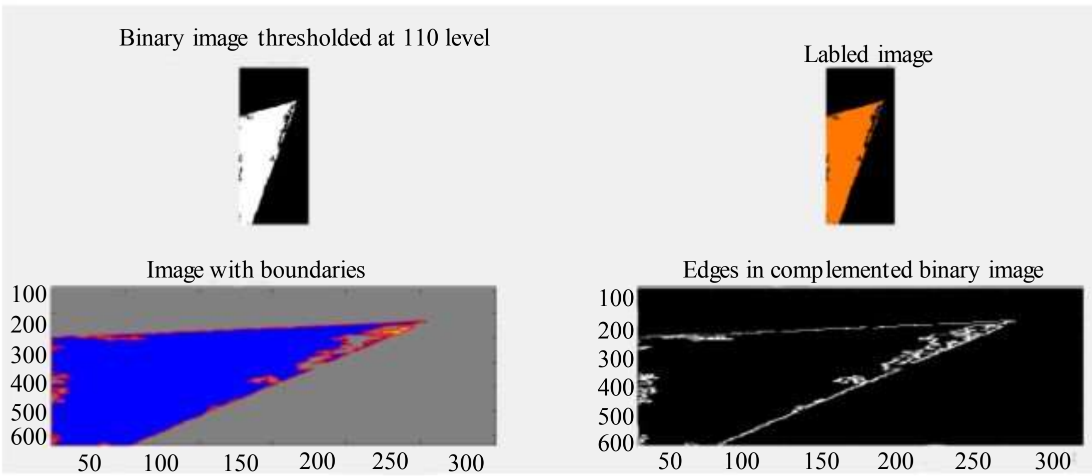

Figure 35. Flank wear MATLAB images for Trial -15.

VB = 0.1mm

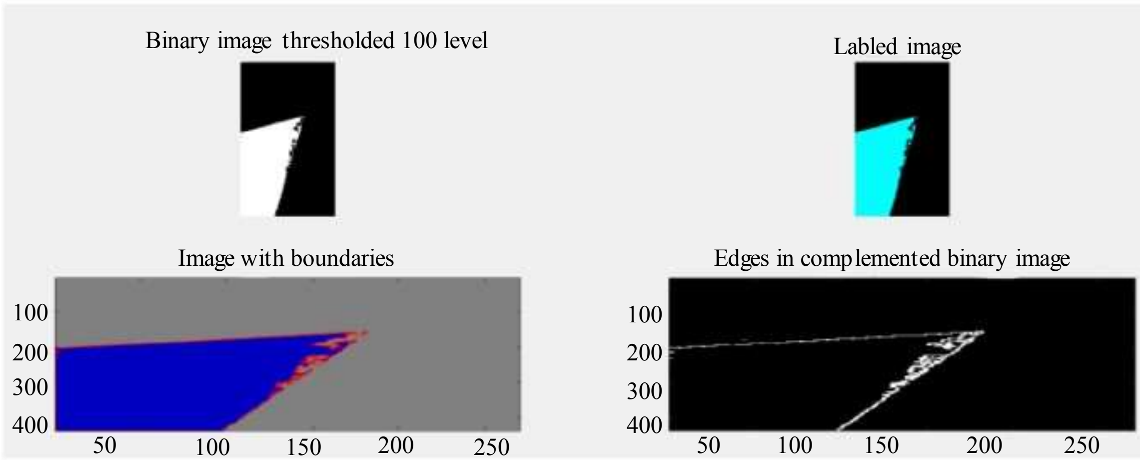

Figure 36. Flank wear MATLAB images for Trial -16.

Flank Wear Results

Table 4 presents the flank wear measurements for tools with a 15° rake angle, derived from MATLAB-based image processing. The observed wear ranged between 0.08 mm and 0.67 mm, with corresponding average values varying from 0.12 mm to 0.46 mm, indicating a noticeable influence of machining conditions on tool degradation.

The results reveal that flank wear increased with higher cutting speeds [14] and feed rates, primarily due to elevated frictional heat and abrasive interaction between the hard Al_2O_3 particles and the HSS tool surface. Tools operating at moderate cutting parameters exhibited lower $V_{B,avg}$ values (≈ 0.16 – 0.25 mm), suggesting enhanced stability and reduced edge attrition. Conversely, higher feeds and speeds promoted micro-abrasive and adhesive wear, leading to accelerated material loss from the flank face.

These findings demonstrate that even a small variation in cutting parameters can significantly affect wear uniformity and surface integrity, highlighting the delicate balance between productivity and tool longevity. From a broader materials perspective, the flank wear progression mirrors interfacial degradation phenomena often encountered in polymer–metal hybrid composites, where local frictional stresses and particle-matrix interactions govern interface durability. Thus, the image-based flank wear quantification provides not only a precise measure of tool reliability but also insights applicable to hybrid composite machining and interface life prediction.

Table 4. Flank wear results for 15º tools.

15 degrees			
Tool type	***VB max (mm)***	***VB min (mm)***	***VB avg (mm)***
Tool_1	0.33	0.16	0.25
Tool_2	0.67	0.18	0.46
Tool_3	0.435	0.13	0.3
Tool_4	0.459	0.157	0.25
Tool_5	0.565	0.12	0.43
Tool_6	0.44	0.134	0.36
Tool_7	0.167	0.08	0.123
Tool_8	0.3	0.1	0.16

Table 5 summarizes the flank-wear characteristics of tools with a 20° rake angle, obtained through MATLAB-based contour and pixel-calibration analysis. The maximum flank-wear values ranged from 0.20 mm to 0.76 mm, while the corresponding average wear varied between 0.135 mm and 0.37 mm. Compared with the 15° tools, a general increase in average wear was observed, indicating that a higher rake angle, although improving chip flow, tends to raise the tool–work contact area and frictional temperature, thereby accelerating wear progression.

Tools subjected to higher cutting speeds and feeds displayed greater $V_{B,avg}$ values due to intensified abrasive interaction between the Al2O3 particulates and the HSS tool flank. In contrast, moderate parameter settings produced smoother chip evacuation and reduced heat accumulation, resulting in more stable wear patterns. The overall wear trend highlights the competing effects of rake geometry: while a larger rake angle enhances cutting efficiency, it can compromise tool life under abrasive composite machining conditions.

From a broader perspective, the wear evolution observed here parallels interface-degradation phenomena in polymer–metal and particulate-reinforced hybrid composites, where the interplay between load transfer, surface temperature, and reinforcement hardness dictates long-term reliability. Thus, quantitative flank-wear evaluation under varying tool geometries provides a robust framework for optimizing both machining performance and interfacial integrity in advanced composite manufacturing.

The above Figure 37 show the variation of tool wear as the rake angle changes. It is observed that for higher rake the wear effect is more. Hence optimum rake is preferred when machining Aluminium alloys.

Table 6 presents the machining observations for Al6063 composites reinforced with Al_2O_3 at varying process parameters. The recorded values include the initial and final workpiece weights, the mass of material removed (W1–W2), and the corresponding machining time for each trial. These data were obtained from the Taguchi L16 orthogonal array experiments and serve as the foundation for evaluating the material removal rate (MRR) and tool performance consistency.

The results reveal noticeable variation in mass removal and machining duration across the 16 trials, reflecting the combined influence of cutting speed, feed rate, and depth of cut. Higher MRR values were associated with elevated speeds and feeds, which enhanced chip formation but also increased cutting temperature and potential tool wear. Conversely, lower machining parameters yielded reduced MRR values but offered better tool stability and dimensional control.

These experimental outcomes confirm the complex trade-off between productivity and tool reliability during the machining of reinforced aluminium composites. The observed trends are analogous to hybrid polymer–metal composite processing, where filler concentration and cutting conditions govern surface finish, interfacial adhesion, and material removal efficiency. Thus, the dataset provides a critical empirical basis for correlating MRR, flank wear, and reliability metrics, leading to a comprehensive understanding of machinability behavior in Al6063–Al_2O_3 systems.

Table 5. Flank wear results of 20º tools.

20 degrees			
Tool type	***VB max (mm)***	***VB min (mm)***	***VB avg (mm)***
Tool_1	0.2	0.09	0.135
Tool_2	0.59	0.14	0.3
Tool_3	0.42	0.12	0.28
Tool_4	0.3	0.1	0.24
Tool_5	0.344	0.17	0.27
Tool_6	0.76	0.1	0.37
Tool_7	0.37	0.07	0.28
Tool_8	0.52	0.11	0.33

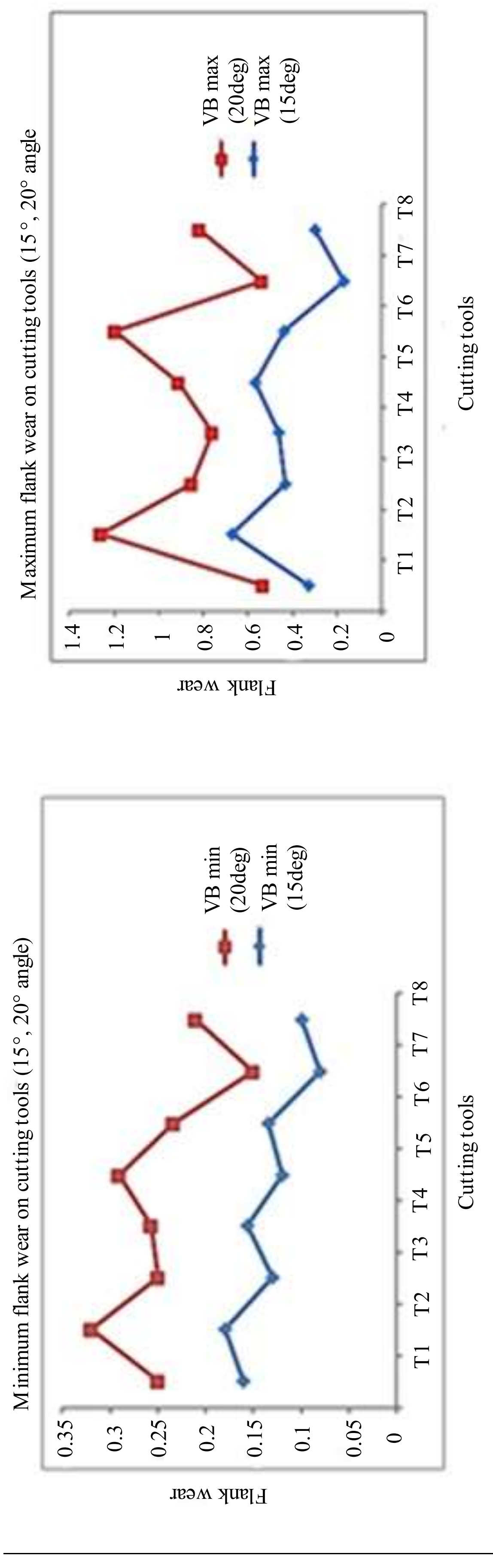

Figure 37. Graphical representation of flank wear for 15^0, 20^0 rake cutting tools.

ISSN: 2321-2810 (Online), ISSN: 2321-8525 (Print)

Table 6. Observations from experimentation for Al_2O_3.

Trail no	Weight before(gms)	Weight after(gms)	W1-W2(gms)	Machining time (s)
1	136.83	135.09	1.74	74
2	135.09	133.29	1.8	81
3	133.29	130.83	2.46	10.3
4	130.83	130.44	0.39	10.6
5	133.78	131.36	2.42	4.5
6	131.36	130.31	1.05	4.79
7	130.31	127.77	2.54	4.97
8	127.77	125.19	2.58	4.89
9	139.35	138.04	1.31	10.6
10	138.04	136.41	1.63	9.64
11	136.41	134.43	1.98	10.45
12	134.43	131.55	2.88	11.41
13	136.85	136.24	0.61	6.77
14	136.24	134.14	2.1	4.58
15	134.14	131.77	2.37	7.5
16	131.77	129.41	2.36	4.87

Table 7. Calculations for Al_2O_3.

Trail no	MRR = (W1-W2)/t	Fx(Kgf)	Fy(Kgf)	Fz(Kgf)	R(Kgf)
1	1.41	-3.00	-6.50	0.00	7.16
2	1.33	-3.00	-6.00	0.00	6.71
3	14.33	-12.25	-40.25	0.00	42.07
4	2.21	-4.00	-19.00	5.50	20.18
5	32.27	-17.50	-63.50	-18.80	68.50
6	13.15	-3.50	-24.00	-15.00	28.52
7	30.66	-16.50	-50.80	-22.60	58.00
8	31.66	-14.00	-45.33	-57.00	74.16
9	7.42	-12.60	-51.08	0.00	52.61
10	10.15	-16.90	-37.89	-19.13	45.68
11	11.37	-14.50	-48.25	-21.58	54.81
12	15.14	-19.00	-65.80	-14.47	70.00
13	5.41	-1.50	-14.60	-10.00	17.76
14	27.51	-16.18	-20.29	-7.83	27.11
15	18.96	-20.50	-108.08	-19.50	111.72
16	29.08	-14.20	-36.07	-11.45	40.42

Experimental Calculations

Table 7 presents the calculated values of Material Removal Rate (MRR), cutting force components (Fx, Fy, Fz), and the resultant cutting force (R) for each trial in the machining of Al6063–Al_2O_3 composites. The MRR was determined from the mass difference between pre- and post-machined specimens, normalized by the machining time. The force components were measured through a lathe-mounted three-axis dynamometer, capturing the real-time mechanical load experienced by the cutting tool during each trial.

The results indicate that MRR values ranged from 1.33 g/s to 32.27 g/s, reflecting the strong influence of machining parameters such as feed rate and cutting speed. The corresponding cutting forces exhibited notable variation, with resultant forces (R) spanning from 6.7 kgf to 68.5 kgf. Higher MRR conditions consistently correlated with increased resultant forces due to the greater mechanical and frictional interaction at the tool–work interface. Conversely, trials with lower MRR values demonstrated reduced cutting loads, signifying stable tool engagement and improved process controllability.

These experimental findings reveal the inherent trade-off between material removal efficiency and tool load intensity, emphasizing those aggressive cutting conditions, while productive, accelerate wear and heat generation. This relationship is analogous to behavior observed in polymer–metal and hybrid composite machining, where processing parameters must be optimized to balance removal efficiency, thermal buildup, and interfacial damage. Consequently, the measured force data serve as a vital input for assessing machining reliability and tool wear modeling, contributing to predictive frameworks for surface integrity and performance in reinforced composite systems.

Reliability Model for Cutting Tool

In the present study, tool reliability analysis was carried out considering the cumulative and simultaneous wear occurring on both the flank and rake faces of the cutting tool. The proposed model is formulated in accordance with the ISO standard wear criterion (VB), focusing primarily on flank wear as the dominant failure mechanism. For reliability evaluation, the cutting tool is assumed to exist in two distinct states, a working (functional) state and a failed (non-functional) state. The transition between these states occurs gradually as the tool undergoes wear, leading to a reduction in cutting efficiency and dimensional accuracy.

From a probabilistic standpoint, the machining process is modeled as a stochastic degradation phenomenon, where the likelihood of tool failure increases with cumulative wear. Excessive flank wear signifies the transition from the working condition to the failure condition [13] [14] [15]. In this study, no catastrophic failures such as cutting-edge fracture or chipping were observed; therefore, tool wear alone was considered the governing failure criterion for reliability estimation.

The following assumptions were made in developing the reliability-based tool-life model:

- The tool wear process is represented as a stochastic hazard function, where each machining event contributes incrementally to cumulative degradation.
- Chemical wear and chipping are modeled as increased hazard contributions due to thermal–chemical interactions at the tool–work interface.
- Infant mortality effects, representing rapid wear during initial tool engagement, are included and modeled as an initially decreasing hazard function.

The model accounts for multiple potential wear mechanisms including flank wear, crater wear, chip notching, groove formation, thermal cracking, softening, diffusion wear, and plastic deformation, though the experimental validation emphasizes flank wear due to its consistent progression across tests. The tool-life distribution is assumed to follow a Normal (Gaussian) distribution, consistent with findings from prior studies on cutting tool reliability.

This reliability formulation enables quantification of the probability of survival (R(t)) and failure rate (λ(t)) of the tool under specific machining conditions. Moreover, the probabilistic framework adopted here parallels approaches used in the reliability analysis of polymer–metal hybrid interfaces and composite joints, where gradual interfacial degradation and fatigue-induced wear dictate service life. Hence, the proposed model provides a generalized methodology applicable not only to metal matrix composite machining but also to multi-material systems, offering insights into the stochastic nature of material–tool or interface wear behavior.

If the average flank wear is the function of feed(f), depth of cut(d), speed(v) and rake angle(r) then,

$$V_B = \emptyset(v, f, d, r)$$

$$\mu = E[V_B] = E[\emptyset(v, f, d, r)]$$

$$\sigma = \backslash textVar[V_B] = E[(V_B - \mu)^2]$$

Journal of Polymer & Composites
Volume 14, Special Issue 2
ISSN: 2321-2810 (Online), ISSN: 2321-8525 (Print)

There is an exponential relationship between flank wear and cutting parameters, thus the flank wear is expressed by

$V_B = C\ v^{b1}\ f^{b2}\ d^{b3}\ r^{b4}$

Where C, b1, b2, b3 are constants which can be obtained from experimentation. Now, the probability density function of flank wear is given by,

$$f(V_b) = \frac{1}{\sqrt{2\pi}\,\sigma} \exp\left(-- \frac{\left(V_b - c_v\ b_1^{b_2}\ d_{b_3}^{b_4}\right)^2}{2\sigma^2} \right)$$

Where VB is the flank wear, μ and σ represents the mean and standard deviation of flank wear respectively.

Damage probability of the flank wear occurred before time t is given by

$$P(\text{rat}) = \int_0^1 r\,dr$$

If the flank wear when the tool life ends is VB*, then the probability of flank wear reach life limit at time t is:

$$P(V_b \geq V) = 1 - \int_0^{V_b} f(V_b)\,dV_b$$

Then,

$$\int_0^1 f(r)\,dr = 1 - \int_0^{V_b} f(V_b)\,dV_b$$

On substituting f(VB), into equation above, rearranging and differentiating with respect to t, we get Probability density function of tool f(t) as

$$f(t) = \frac{1}{\sqrt{2\pi}\sigma} \exp\left[-\frac{(T_v - t)^2}{2\sigma^2} \right]$$

Whereas, TV is the time when average flank wear reach VB* value. Reliability function R(t) can be obtained from the following equation.

However, there is no closed form of solution to this integral, then the transformation Z is given by,

Therefore, in general the reliability equation of cutting tool based on the failure phenomenon is given by

$$R(t) = 1 - P(T < t)$$

$$R(t) = 1 - \int_{-\infty}^{t} \frac{1}{\sqrt{2\pi}\sigma} \exp\left(-\frac{1}{2}\left(\frac{x-\mu}{\sigma}\right)^2 \right) dx$$

$$R(t) = 1 - \Phi\left(\frac{T_v - \mu}{\sigma}\right)$$

$$Z = \frac{T_v - \mu}{\sigma}$$

$$R(t) = 1 - \Phi(Z)$$

Thus, R(t) = 1-ϕ(Z)Where ϕ (Z) is the probability of failure of the tool. Hence R(t) = 1 - P(t) Value of Z is chosen from Normal Distribution Table.

CONCLUSIONS

The experimental investigation and reliability analysis of HSS single-point cutting tools during the machining of $Al6063–Al_2O_3$ composites led to the following conclusions:

1. For the 15° rake-angle tool, the highest reliability of 99% was achieved at a material removal rate (MRR) of 2.21 g/s corresponding to a resultant cutting force of 20.18 kgf, indicating stable tool–work interaction under moderate machining conditions.
2. The lowest reliability of 83.8% for the same tool geometry occurred at an MRR of 30.66 g/s and a resultant force of 58 kgf, reflecting the adverse effect of aggressive cutting on tool stability and wear progression.
3. For the 20° rake-angle tool, the minimum reliability of 3.09% was recorded at an MRR of 27.51 g/s and a resultant force of 27.11 kgf, signifying rapid degradation under high material-removal conditions.
4. The maximum reliability of 95.67% for the 20° tool was observed at an MRR of 15.14 g/s and a resultant force of 70 kgf, demonstrating that optimized combinations of rake geometry and process parameters can sustain longer tool life.
5. Overall, it was observed that lower MRR values correspond to higher tool reliability for both rake-angle configurations, confirming the inverse relationship between productivity and tool durability.
6. In general, machining with a higher feed and lower cutting speed combination yielded superior reliability, while lower feed and higher speed combinations led to accelerated wear and reduced tool life.

These findings establish that the reliability of HSS tools in machining reinforced aluminium composites is strongly dependent on the balance between mechanical loading and heat generation. The observed trends are consistent with wear–fatigue phenomena in polymer–metal hybrid composites, where interfacial stability and surface degradation dictate service life. The proposed reliability model and experimental correlations thus provide a quantitative foundation for optimizing machining and processing parameters in both metal- and polymer-based composite systems.

Acknowledgements

This project is funded by Institution of Engineers, India (IEI). Institution of Engineers is a Professional body established in 1920 that works for advancement in all engineering disciplines by conducting Conferences, training programs, workshops, faculty development programs and also sponsors research projects to promote R&D activities.

REFERENCES

1. J.G. Wager, M.M. Barash, (1971) “Study for distribution of the life of HSS tools”, Journal of Engineering for Industry, ASME 73/4 295-299.
2. K. Hitomi, N. Nakamura, S. Inoue, (1979) “Reliability analysis of cutting tools”, Journal of Engineering for Industry 101 185-190.
3. W.S. Lin, (2008) “The reliability analysis of cutting tools in the HSM processes”, International Scientific Journal published monthly by the World Academy of Materials and Manufacturing Engineering, Volume 30 Issue 2 Pages 97-100.
4. El Wardany, T. I., & Elbestawi, M. A. (1997). Prediction of tool failure rate in turning hardened steels. The International Journal of Advanced Manufacturing Technology, 13(1), 1–16. doi:10.1007/bf01179225
5. Konstantinos Salonitisa, Athanasios Koliosb, (2013) “Reliability assessment of cutting tools life based on advanced approximation methods”, ScienceDirect.
6. Carmen Elena Patino Rodriguez, Gilberto Francisco Martha de Souza, (2013) “Reliability concepts applied to cutting tool change time”, IJSRK.

7. S. Ajmal Hussain, Rajaneesh R, Hashim Nizam, Jithin K (2019) “Experimental Analysis on Aluminum alloy (6063) with Silicon Carbide: An Experimental Investigation”, Volume: 06, IRJET
8. Siva Bhaskar, Venkata Ramesh Mamilla, (2013) “A Reliability Based Approach for Predicting Optimal Tool Replacement Time,” International Journal of Scientific Research in Knowledge.
9. Oussama Zerti, Athmane Yallese, Salim Belhadi, Lakhdar Bouzid, (2014) “Taguchi Design of Experiments for Optimization and Modeling of Surface Roughness When Dry Turning X210Cr12 Steel”, ResearchGate.
10. Nithin M Mali, T. Mahender, (2015) “Wear Analysis of Single Point Cutting Tool with And Without Coating”, International Journal of Research in Engineering and Advanced Technology, Volume 3, Issue 3.
11. Abdullah Hassan Mihdy Jassim, (2015) “Effect of Heat Treatments on the Tensile Properties and Impact Toughness of 6063 Aluminium Alloy”, ResearchGate.
12. Kwon, W. T., Park, J. S., & Kang, S. (2005) “Effect of group IV elements on the cutting characteristics of Ti (C, N) cermet tools and reliability analysis”, Journal of Materials Processing Technology, 166(1), 9–14.
13. Montasser S. Tahat, Nadim A. Emira, Hamzeh T. Mohamad, (2010) “Study of the Mechanical Properties of Heat Treated 6063 Aluminium Alloy”, ResearchGate.
14. U. Lakshiminarayana, B. Sri Harsha Vardhan Reddy, K. Srinu, B. SurBabu, Akula Siva Bhaskar, (2015) “Predicting Optimal Tool Replacement Time in Turning of Super Alloy Using Reliability Testing”, Journal of Material Science and Mechanical Engineering, Volume 2, Number 5.
15. Vishal S. Sharma, S. K. Sharma, Ajay K. Sharma, (2007) “Cutting Tool Wear Estimation for Turning.” Springer.
16. S. G. J. G. K. a. P. P. Epstein, " Aluminum And Its Alloys," in *Mechanical Engineers' Handbook*, Washington, DC, The Aluminum Association, Inc, 1994, p. 14.
17. J. M. Runge, " Metallurgy Basics for Aluminum Surfaces," in *The Metallurgy of anodizing aluminum*, Chicago, IL, USA, Springers, 2018, p. 433.
18. Raj Kumar, Dr. Vineet, "Optimization Of Process Parameter For Stir Casted Aa6063 Metal Matrix Composite On Hardness, Tensilestrength And Impact Energy," *International Journal of Mechanical Engineering and Technology (IJMET),* vol. 9, no. International Journal of Mechanical Engineering and Technology, p. 9, December 2017.
19. A.A.S. Metals. Inc, "Asm. Matweb," [Online]. Available: https://asm.matweb.com/search/GetReference.asp?bassnum=MA6063T6.
20. A. International, Metals Handbook, Vol.2 - Properties and Selection: Nonferrous Alloys and Special-Purpose Materials, ASM International, 1990.

